Computers and Chemical Engineering 104 (2017) 296–310

Contents lists available at ScienceDirect

Computers and Chemical Engineering

journal homepage: www.elsevier.com/locate/compchemeng

Optimization formulations for multi-product supply chain networks

Apoorva M. Sampat[a], Edgar Martin[b], Mariano Martin[b], Victor M. Zavala[a,*]

[a] Department of Chemical and Biological Engineering, University of Wisconsin-Madison, 1415 Engineering Dr, Madison, WI 53706, USA
[b] Department of Chemical Engineering, University of Salamanca, Plz. Caidos 1-5, 37008 Salamanca, Spain

ARTICLE INFO

Article history:
Received 4 February 2017
Received in revised form 6 April 2017
Accepted 22 April 2017
Available online 4 May 2017

Keywords:
Multi-product
Graph
Supply chain
Priorities
Multi-stakeholders
Organic waste

ABSTRACT

We present optimization formulations for multi-product supply chain networks. The formulations use a general graph representation that captures dependencies between an arbitrary number of products, technologies, and transportation paths. We discuss how to use the framework to compute compromise solutions that resolve geographical and stakeholder conflicts. We present case studies in which we seek to design supply chains to collect and process organic waste from a large number of farms in the State of Wisconsin to mitigate point phosphorus and methane emissions.

1. Introduction

Multi-product supply chain networks involve a set of products that are transported to geographically dispersed facilities to be transformed into intermediate and final products that are delivered to final destinations. These models are used to identify optimal facility types, sizes, and locations (network design) as well as to identify optimal resource allocation strategies (network management/operation) (Bloemhof-Ruwaard et al., 1996; Guillén-Gosálbez and Grossmann, 2009; You et al., 2012, 2009; Kim et al., 2008; Neiro and Pinto, 2004; Papageorgiou et al., 2001; Grossmann, 2004). Coupled infrastructure networks (e.g., gas, electric, water) as well as chemical supply chains are important application areas. The presence of *product transformations* is a key feature that distinguishes these models from those arising in other domains such as multi-commodity network flows (Hu, 1963).

The agricultural industry is an important application area of supply chain models. Models have been recently developed for biomass-to-fuels supply chains for the conversion of food crops to biodiesel (You and Grossmann, 2008a,b; Mele et al., 2011; Giarola et al., 2011; Zamboni et al., 2009; Akgul et al., 2010; Corsano et al., 2011), cellulosic biomass to biodiesel (Alex Marvin et al., 2012; Eksioglu et al., 2009; Čuček et al., 2010; Huang et al., 2010; Leduc et al., 2010; Dal-Mas et al., 2011; Santibañez-Aguilar et al., 2011; Akgul et al., 2012; Chen and Fan, 2012; Chen, 2014), cellulosic biomass to general biofuels (Parker et al., 2010; Tittmann et al., 2010; Bowling et al., 2011; Kim et al., 2011a,b; Papapostolou et al., 2011; You and Wang, 2011; Walther et al., 2012), algae to biofuels (Avami, 2012), and biomass to energy (Elia et al., 2011; Dunnett et al., 2007; Dawoud et al., 2007; Burak Aksoy et al., 2011; Čuček et al., 2012). Recent studies have also pointed out the need to model complex interactions over a wider range of products that include food, water, and energy resources (Garcia and You, 2016; Čuček et al., 2014).

In this work, we present optimization formulations for multi-product supply chain networks. The formulations use a general network representation that captures dependencies between an arbitrary number of products, technologies, and transportation paths. Interactions between products are captured by using a *hierarchical graph* that maps products at each node using a transformation matrix and that maps network nodes by using transportation links (arcs). The proposed graph abstraction combines modeling concepts from supply chain and infrastructure networks. With this, we seek to provide a formal and general representation that can capture a wide range of settings existing in the literature (which tend to be developed on a case-by-case basis). For instance, the formulations presented in Bowling et al. (2011), Hugo and Pistikopoulos (2005), Kalaitzidou et al. (2015) and You et al. (2012) capture interactions between multiple products but no general representation is provided. Our abstraction also makes an explicit distinction between in-network (derived) product flows and out-of-network source (supply) and sink (demand)

* Corresponding author.
E-mail address: victor.zavala@wisc.edu (V.M. Zavala).

http://dx.doi.org/10.1016/j.compchemeng.2017.04.021
0098-1354/

product flows. This feature can be used to couple boundaries of different systems and to derive internal prices (for intermediate products) in a more systematic manner, compared to existing models (Alex Marvin et al., 2012; An et al., 2011; Balaman and Selim, 2014; Kim et al., 2011b). Our graph abstraction resembles that used in p-graphs (Varbanov and Friedler, 2008; Lam et al., 2010) in which nodes are interpreted as technologies (unit operations) that transform products. The p-graph abstraction enables the use of graph-theoretical strategies to identify feasible pathways between products and feasible network topologies (i.e., superstructures) (Varbanov and Friedler, 2008) as well as to design supply chains (Čuček et al., 2010). Our proposed abstraction extends this work by using a general optimization setting that includes more complex sets of constraints and objectives. In particular, we show how to use the formulations to capture conflicting priorities on different metrics and geographical network locations. We demonstrate the applicability of the proposed framework by using a case study in the State of Wisconsin, in which we seek to design supply chains to process organic waste from a set of concentrated animal feeding operations (CAFOs) to mitigate point phosphorus and methane emissions.

The paper is structured as follows. In Section 2 we introduce the proposed multi-product network abstraction. In Section 3 we discuss how this framework can be used to derive high-level optimization formulations. In Section 4 we apply the proposed framework to case studies that seek to perform phosphorus and biogas recovery from agricultural organic waste across the State of Wisconsin. The paper closes in Section 5 with conclusions and directions for future work.

2. Multi-product network modeling

We consider a network (a graph) that comprises a set of nodes $\mathcal{N}$, links (arcs) $\mathcal{F}$, products $\mathcal{P}$, out-of-network sources $\mathcal{S}$, and out-of-network sinks $\mathcal{D}$. Associated with each link $\ell \in \mathcal{F}$, there is a *one-directional* flow $f_\ell \in \mathbb{R}_+$ (where $\mathbb{R}_+$ is the non-negative orthant) that has the following attributes: product type $prod\_link[\ell] \in \mathcal{P}$, capacity $cap\_link[\ell] \in \mathbb{R}_+$, transportation cost $cost\_link[\ell] \in \mathbb{R}_+$, sending node $snd\_link[\ell] \in \mathcal{N}$, and receiving node $rec\_link[\ell] \in \mathcal{N}$. We use attributes to define subsets and nested set partitions. In particular, the set $\mathcal{F}_n^{in}:=\{\ell | rec\_link[\ell]=n\}$ is the set of all flows entering node $n \in \mathcal{N}$. Similarly, the set $\mathcal{F}_n^{out}:=\{\ell | snd\_link[\ell]=n\}$ is the set of all flows leaving node $n \in \mathcal{N}$. We also define the nested subsets for entering flows $\mathcal{F}_{n,p}^{in} \subseteq \mathcal{F}_n^{in} \subseteq \mathcal{F}$ where $\mathcal{F}_{n,p}^{in}:=\{\ell | rec\_link[\ell]=n, prod\_link[\ell]=p\}$ and note that $\cup_{p\in\mathcal{P}}\mathcal{F}_{n,p}^{in}=\mathcal{F}_n^{in}$. We use similar definitions to construct subsets for the leaving flows $\mathcal{F}_{n,p}^{out} \subseteq \mathcal{F}_n^{out} \subseteq \mathcal{F}$.

Associated with each out-of-network source $i \in \mathcal{S}$ is a flow $s_i \in \mathbb{R}_+$ with attributes: product type $prod\_src[i] \in \mathcal{P}$, source capacity $\bar{s}_i:=cap\_src[i] \in \mathbb{R}_+$, node $node\_src[i] \in \mathcal{N}$, and cost $\alpha_i^s:=cost\_src[i] \in \mathbb{R}_+$. Similarly, associated with each out-of-network sink $j \in \mathcal{D}$ is a flow $d_j \in \mathbb{R}_+$ with attributes: product type $prod\_sink[j] \in \mathcal{P}$, sink capacity $\bar{d}_j:=cap\_sink[j] \in \mathbb{R}_+$, node $node\_sink[j] \in \mathcal{N}$, and cost $\alpha_j^d:=cost\_sink[j] \in \mathbb{R}_-$ (where $\mathbb{R}_-$ denotes the non-positive orthant). We again use attributes to define the nested sets $\mathcal{S}_{n,p} \subseteq \mathcal{S}_n \subseteq \mathcal{S}$ with $\mathcal{S}_n:=\{i | node\_src[i]=n\}$ (i.e., all sources attached to a node n) and $\mathcal{S}_{n,p}:=\{i | node\_src[i]=n, prod\_src[i]=p\}$ (i.e., all sources of product p attached to node n). We can follow a similar reasoning to define the nested sets $\mathcal{D}_{n,p} \subseteq \mathcal{D}_n \subseteq \mathcal{D}$.

Associated with each node $n \in \mathcal{N}$ there are transformation factors $\gamma_{n,p} \in \mathbb{R}, p \in \mathcal{P}$ and attributes: reference *input* product $p'(n):=refprod\_node[n] \in \mathcal{P}$ and capacity $\bar{g}_n:=cap\_node[n] \in \mathbb{R}_+$. The transformation factors are expressed as units of product p consumed/generated per unit of reference product $p'(n)$ consumed/generated at a given node. We use the convention that $\gamma_{n,p} > 0$ if product p is generated in node n, $\gamma_{n,p} < 0$ if product p is consumed in node n, and $\gamma_{n,p} = 0$ if product p is neither produced nor consumed in node n. Associated with each node is also a production flow for each product $g_{n,p} \in \mathbb{R}$ with an associated production cost $\alpha_{p,n}^g \in \mathbb{R}$. We use the convention that $\text{sgn}(\gamma_{n,p}) = \text{sgn}(\alpha_{p,n}^g)$ to indicate that, if a product is generated, then it becomes an *in-network* supply product with a positive cost and, if it is consumed, then it becomes an *in-network* demand product with a negative cost. The notation and node-level interactions are sketched in Fig. 1.

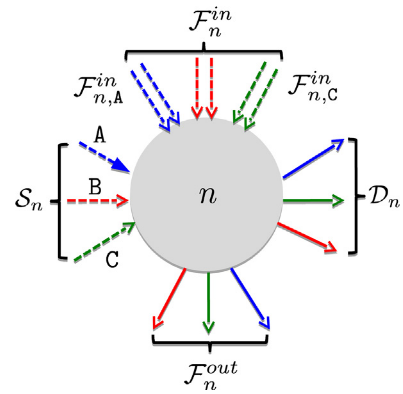

Fig. 1. Sketch of input and output flow sets into node n for products A, B, C.

Using these basic definitions we impose the following product balances at each node $n \in \mathcal{N}$ in the network:

$$\left(\sum_{i\in\mathcal{S}_{n,p}} s_i + \sum_{\ell\in\mathcal{F}_{n,p}^{in}} f_\ell\right) - \left(\sum_{j\in\mathcal{D}_{n,p}} d_j + \sum_{\ell\in\mathcal{F}_{n,p}^{out}} f_\ell\right) + g_{n,p} = 0, (n,p) \in \mathcal{N}\times\mathcal{P}. \tag{2.1}$$

The first term in parenthesis is the total input flow for product p (given by supply flows and links entering the node). The second term in parenthesis is the total output flow of product p (given by the demand flows and links leaving the node). The third therm is the generation/consumption flow of product p. The notation and network-level interactions are sketched in Fig. 2.

The total input flow of the reference product $p'(n)$ in node n (both inflows and out-of-network sources) are split into a processed and unprocessed input flow $r_{n,p'(n)} \in \mathbb{R}_+$ and $u_{n,p'(n)} \in \mathbb{R}_+$, respectively. This is modeled as:

$$\left(\sum_{i\in\mathcal{S}_{n,p'(n)}} s_i + \sum_{l\in\mathcal{F}_{n,p'(n)}^{in}} f_\ell\right) = r_{n,p'(n)} + u_{n,p'(n)}, n \in \mathcal{N}. \tag{2.2}$$

The generation/consumption of product p is expressed in terms of the reference product $p'(n)$ as:

$$g_{n,p} = \gamma_{n,p} r_{n,p'(n)}, (n,p) \in \mathcal{N}\times\mathcal{P}. \tag{2.3}$$

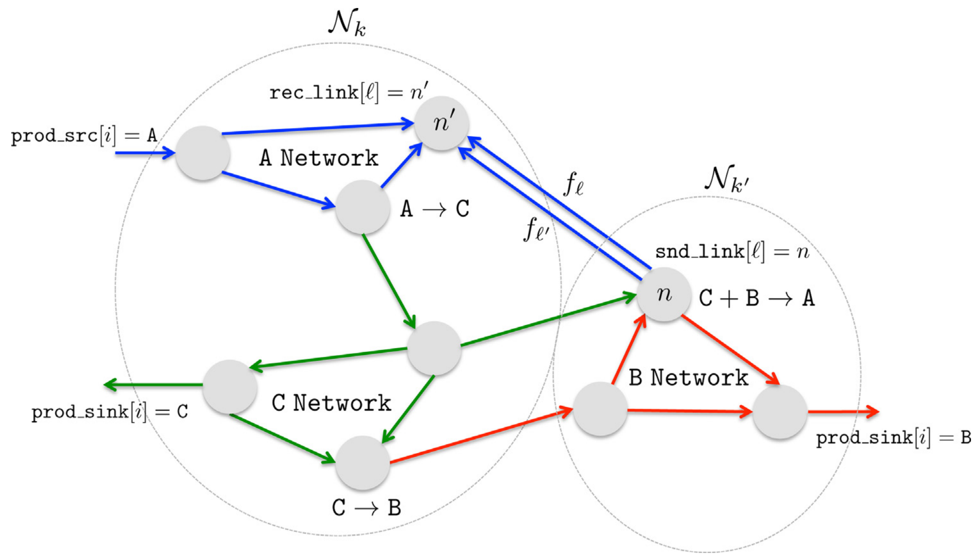

Fig. 2. Sketch of multi-product network coupling and notation.

We note that Eqs. (2.1), (2.3), and (2.2) can be combined to give:

$$\left(\sum_{i\in\mathcal{S}_{n,p}} s_i + \sum_{\ell\in\mathcal{F}^{in}_{n,p}} f_\ell\right) - \left(\sum_{j\in\mathcal{D}_{n,p}} d_j + \sum_{\ell\in\mathcal{F}^{out}_{n,p}} f_\ell\right) + \gamma_{n,p} r_{n,p'(n)} = 0, (n,p)\in\mathcal{N}\times\mathcal{P} \tag{2.4}$$

or,

$$\left(\sum_{i\in\mathcal{S}_{n,p}} s_i + \sum_{\ell\in\mathcal{F}^{in}_{n,p}} f_\ell\right) - \left(\sum_{j\in\mathcal{D}_{n,p}} d_j + \sum_{\ell\in\mathcal{F}^{out}_{n,p}} f_\ell\right) + \gamma_{n,p}\left(\sum_{i\in\mathcal{S}_{n,p'(n)}} s_i + \sum_{\ell\in\mathcal{F}^{in}_{n,p'(n)}} f_\ell\right) = \gamma_{n,p} u_{n,p'(n)}, (n,p)\in\mathcal{N}\times\mathcal{P}. \tag{2.5}$$

From these expressions it becomes clear that individual product networks couple at the nodes. We can also see that the transformation factors $\gamma_{n,p}$ measure the strength of the coupling between networks (by setting $\gamma_{n,p}=0$ we decouple the networks). The balance for reference product $p'(n)$ can also be expressed as:

$$(1+\gamma_{n,p'(n)})\left(\sum_{i\in\mathcal{S}_{n,p'(n)}} s_i + \sum_{\ell\in\mathcal{F}^{in}_{n,p'(n)}} f_\ell\right) - \left(\sum_{j\in\mathcal{D}_{n,p'(n)}} d_j + \sum_{\ell\in\mathcal{F}^{out}_{n,p'(n)}} f_\ell\right) = \gamma_{n,p'(n)} u_{n,p'(n)}, n\in\mathcal{N}. \tag{2.6}$$

We can thus see that $\gamma_{n,p'(n)} \geq -1$ must hold and we see that the unprocessed flow $u_{n,p'(n)}$ represents the net (residual) flow of the reference product in the node. The processed and unprocessed flow constraints at the nodes are given by:

$$0 \leq u_{n,p'(n)}, n\in\mathcal{N}, \tag{2.7a}$$

$$0 \leq r_{n,p'(n)} \leq |1\backslash\gamma_{n,p'(n)}|\bar{g}_n, \quad n\in\mathcal{N}. \tag{2.7b}$$

From (2.3) we note that the later constraint is equivalent to $0 \leq |g_{n,p'(n)}| \leq \bar{g}_n, n\in\mathcal{N}$.

Capacities on flows as well as out-of-network sources and sinks are given by:

$$0 \leq f_\ell \leq \bar{f}_\ell, \ell\in\mathcal{F}, \tag{2.8a}$$

$$0 \leq s_i \leq \bar{s}_i, i\in\mathcal{S}, \tag{2.8b}$$

$$0 \leq d_j \leq \bar{d}_j, j\in\mathcal{D}. \tag{2.8c}$$

We highlight some key features of the proposed abstraction. The products can be interpreted as primary or derived products such as natural gas, electricity, sensor information, raw and derived chemical products, pollutants, water, or streams of different quality that come from the network boundary (i.e., out-of-network) or from the network (i.e., in-network). Products induce a hierarchy of primary, secondary, and final products at the nodes (e.g., biomass to biodiesel to carbon dioxide) directly from the transformation factors $\gamma_{n,p}$ or implicitly through the network. The supply flows s_i are *out-of-network* suppliers while $g_{n,p}$ (with positive sign) are *in-network* supply flows. In other words, out-of-network supplies are not produced at the nodes but enter the system for its boundaries. Similarly, d_j are out-of-network demands while $g_{n,p}$ (with negative sign) are in-network demands. Nodes are interpreted as individual technologies (pieces of equipment or entire facilities) that perform physico-chemical transformations (e.g., chemical plants, separators, power plants, heat exchangers, biodigesters, storages, compressor, pumps). The transformation factors can be used to specify chemical reactions (induced or due to degradation), split factors, or storage efficiencies to model losses or gains due to interactions with the environment.

In-network production flows $g_{n,p}$ are expressed as a function of the reference product and are defined by $\gamma_{n,p}$ (i.e., units of p produced per unit of reference product $p'(n)$). For nodes that do not perform transformations we set $\gamma_{n,p}=0$ and they become simple transportation/transshipment nodes. The cost factors for suppliers, demands can be interpreted as *offering prices* for products at different locations (nodes) and we note that there might be multiple suppliers and demands of the same product to a single node. Cost factors for production flows can be used to capture offering/supply costs for products in different technologies (e.g., different technologies can generate a product at different costs). Cost factors for flows can be interpreted as offering prices for transportation services for a given link (or can be used to capture other features such as transportation delays). We note that multiple links can exist between nodes with different transportation costs (to reflect the possibility that different types of transportation or links of the same type are available). We thus seek to highlight that the proposed modeling abstraction is general and flexible.

2.1. Degrees of freedom

We define $N = |\mathcal{N}|$, $F = |\mathcal{F}|$, $P = |\mathcal{P}|$, $L = |\mathcal{F}|$, $S = |\mathcal{S}|$, and $D = |\mathcal{D}|$ (where $|\cdot|$ denotes the cardinality of the set). The total number of variables is given as follows: for flows f_ℓ is F, for sources s_i is S, for sinks d_j is D, and for processed and unprocessed input flow $r_{n,p'(n)}$, $u_{n,p'(n)}$ is $2N$ (by noticing that $g_{n,p}$ can be expressed in terms of $r_{n,p'(n)}$ alone). This gives a total of $2N+F+S+D$ variables. The total number of equations is: for node balances (2.1) is $N \cdot P$ and for the split equations (2.2) is N. This gives a total of $N(P+1)$ equations. The total number of degrees of freedom is $2N+F+S+D-NP-N$. Consequently, these many variables need to be specified for the network to be fully defined.

If we define a source and a sink per node and per product (i.e., $S=D=NP$), the number of degrees of freedom is $2N+F+NP+NP-NP-N=N+F+NP=N(P+1)+F$. Consequently, in addition to specifying all the flows, we need to specify $N(P+1)$ sinks or sources for the system to be fully defined. In the single product case (i.e., $P=1$), we would need to specify the $2N$ sinks or sources in addition to the flows to fully define the system. We also note that the number of flows connecting the nodes can be extremely large. For instance, if we consider that a flow can exist between any pair of nodes, for every product, and in every direction, but no self-flows are allowed (i.e., $f_\ell=0$ for `snd_link[`ℓ`]=rec_link[`ℓ`]`) we have $F=2N(N-1)\cdot P$ flow variables. This shows a quadratic growth in complexity with the number of network nodes. For instance, a network with $O(10^2)$ nodes has $O(10^4)$ possible flows.

2.2. Transportation nodes and decoupled networks

For a given product p, the balance equation at node n with no generation/consumption ($\gamma_{n,p}=0$) is:

$$\left(\sum_{i\in\mathcal{S}_{n,p}} s_i + \sum_{\ell\in\mathcal{F}^{in}_{n,p}} f_\ell\right) - \left(\sum_{j\in\mathcal{D}_{n,p}} d_j + \sum_{\ell\in\mathcal{F}^{out}_{n,p}} f_\ell\right) = 0,\ n \in \mathcal{N}. \quad (2.9)$$

The node becomes a simple transportation node for product p. The case with $\gamma_{n,p}=0$ for all $n \in \mathcal{N}$ and $p \in \mathcal{P}$ indicates also that there is no product transformation at any node, and the balance equations become:

$$\left(\sum_{i\in\mathcal{S}_{n,p}} s_i + \sum_{\ell\in\mathcal{F}^{in}_{n,p}} f_\ell\right) - \left(\sum_{j\in\mathcal{D}_{n,p}} d_j + \sum_{\ell\in\mathcal{F}^{out}_{n,p}} f_\ell\right) = 0,\ (n,p) \in \mathcal{N}\times\mathcal{P}. \quad (2.10)$$

This indicates that the individual product networks decouple, as is the case of multi-commodity network flow models (i.e., the proposed representation can capture this case as well). This situation also arises in electrical, gas, and electrical network models when interdependencies are ignored.

3. Optimization formulations

We now illustrate how to incorporate the proposed framework into high-level optimization problems of interest in network design.

3.1. Network operations

The resource allocation problem is a classical problem in supply chain optimization that seeks to capture operational performance (in the form of economics, environmental, or social objectives). To define this problem using the proposed notation, we consider supply cost, demand cost, generation/consumption cost, and transportation cost for each element of the network:

$$\varphi^d_j = \alpha^d_j d_j,\ j \in \mathcal{D}, \quad (3.11a)$$

$$\varphi^s_i = \alpha^s_i s_i,\ i \in \mathcal{S}, \quad (3.11b)$$

$$\varphi^f_\ell = \alpha^f_\ell f_\ell,\ \ell \in \mathcal{F}, \quad (3.11c)$$

$$\varphi^g_{n,p} = \alpha^g_{n,p} g_{n,p},\ (n,p) \in \mathcal{N}\times\mathcal{P}. \quad (3.11d)$$

This gives rise to the multi-objective allocation problem:

$$\min\{\varphi^d_j, \varphi^s_i, \varphi^f_\ell, \varphi^g_{n,p}\} \quad (3.12a)$$

$$\text{s.t.}\quad (2.1),\quad (2.7),\quad (2.8). \quad (3.12b)$$

This formulation seeks to capture inherent trade-offs between revenue collected from individual sources, cost incurred by sinks (consumers), revenue/costs of in-network suppliers/consumers (technology provides), and revenue of transportation providers. Here, we assume that each supplier, demand, flow, and technology provider represents a different objective. This allows us to capture natural conflicts among network locations. Consequently, this problem can be interpreted as a market clearing problem(Pritchard et al., 2010; Zavala et al., 2017).

In summary, the statement of the network operation problem is: Given a set of products ($\mathcal{P}$), sources ($\mathcal{S}$), sinks ($\mathcal{D}$), and nodes ($\mathcal{N}$), the goal is to determine an optimal allocation of flows (f_ℓ), product supplies (s_i), and demands (d_j) that constitute a Pareto optimal solution of the problem (3.12).

3.1.1. Prioritization

Traditionally, a compromise (Pareto) solution for the multi-objective problem is found by maximizing the social welfare function:

$$\varphi = \underbrace{\sum_{j\in\mathcal{D}} \varphi^d_j}_{\varphi_d} + \underbrace{\sum_{i\in\mathcal{S}} \varphi^s_i}_{\varphi_s} + \underbrace{\sum_{\ell\in\mathcal{F}} \varphi^f_\ell}_{\varphi_f} + \underbrace{\sum_{(n,p)\in\mathcal{N}\times\mathcal{P}} \varphi^g_{n,p}}_{\varphi_g}. \quad (3.13)$$

This formulation implicitly seeks to maximize the demand served while minimizing supply and transportation costs (recall that cost coefficients for in-network and out-of-network demand flows are negative). One can easily show that the solution of this problem is a Pareto optimal solution of problem (3.12). Moreover, the coefficients $\alpha^s_i, \alpha^d_j, \alpha^f_\ell, \alpha^g_{n,p}$ are used to prioritize different node locations and often have natural economical interpretations (i.e., offering prices).

We also note that a solution of the social welfare problem is a Pareto optimal solution of the aggregated problem:

$$\min\{\varphi^d, \varphi^s, \varphi^f, \varphi^g\} \quad (3.14a)$$

$$\text{s.t.}\quad (2.1),\quad (2.7),\quad (2.8) \quad (3.14b)$$

in which we capture trade-offs between *total* supply, demand, transportation, and production costs. It is also well-known that a Pareto optimal solution to this problem can be found by using an ϵ-constrained method. In this approach we solve problems of the form:

$$\min \varphi^d \tag{3.15a}$$

$$\text{s.t.} \quad (2.1), \quad (2.7), \quad (2.8) \tag{3.15b}$$

$$\varphi^s \le \epsilon^s, \varphi^f \le \epsilon^f, \varphi^g \le \epsilon^g, \tag{3.15c}$$

where ϵ^s, ϵ^f, ϵ^g are threshold values. We note that we have picked (arbitrarily and without loss of generality) the demand cost as the cost to be minimized. It is also possible to derive ϵ-constrained formulations by using the individual node costs but this would result in an extremely large number of threshold values to be specified. Because of this, it is often difficult to identify threshold values under which a feasible solution exists.

3.1.2. Multi-stakeholder prioritization

In certain settings, the coefficients α_i^s, α_j^d, α_ℓ^f, $\alpha_{n,p}^g$ do not have well-defined values. This can be because markets for certain products (e.g., agricultural or food waste) are not well-established or because different decision-makers (e.g., government agencies or facility managers) attribute different importance to different geographical locations. In such cases, it is possible to rely on *opinions* from multiple stakeholders that seek to express their priorities and to use such opinions to identify compromise solutions for the multi-objective problem (3.12).

Consider the situation in which a stakeholder $\omega \in \Omega$ prioritizes the total cost vector $\varphi = (\varphi_d, \varphi_s, \varphi_f, \varphi_g)$ by using the weight vector $\mathbf{w}_\omega$ to construct the scalar function $\mathbf{w}_\omega^T \varphi$. The optimal solution for this stakeholder is thus given by:

$$f_\omega := \min \mathbf{w}_\omega^T \varphi \tag{3.16a}$$

$$\text{s.t.} \quad (2.1), \quad (2.7), \quad (2.8). \tag{3.16b}$$

Here, f_ω is the optimal objective for the stakeholder ω given her/his priority vector and represents the situation in which the stakeholder is *most satisfied*. Stakeholders, however, will naturally disagree on how to prioritize the different objective functions. Consequently, we define a dissatisfaction function that will measure how dissatisfied is stakeholder $\omega \in \Omega$ with an alternative solution that is not optimal for her/his priorities (i.e., it is not the solution of (3.16)). The dissatisfaction function is given by $d_\omega = \mathbf{w}_\omega^T \varphi - f_\omega$. A compromise solution for the stakeholders can thus be found by minimizing a measure of the dissatisfactions $d_\omega, \omega \in \Omega$. In Dowling et al. (2016) it is proposed to use the conditional value at risk (CVaR) as a *collective dissatisfaction measure* that we seek to minimize. The resulting problem is given by:

$$\min \nu + \frac{1}{\beta|\Omega|} \sum_{\omega \in \Omega} [d_\omega - \nu]_+ \tag{3.17a}$$

$$\text{s.t.} \quad (2.1), \quad (2.7), \quad (2.8), \tag{3.17b}$$

where $\beta \in (0, 1]$ is a probability level and ν is the value at risk. One can show that this problem minimizes the worst dissatisfaction when $\beta \to 0$ and it minimizes the average collective dissatisfaction when $\beta = 1$. Moreover, one can show that the solution of the CVaR problem are Pareto optimal for (3.12).

In the proposed setting, the stakeholders prioritize supply, demand, generation, and transportation costs. The multi-stakeholder framework, however, is general and can also be used to find compromise solutions for stakeholders prioritizing individual nodes (or regions) and products. We also highlight that the computation of the compromise solution does not require the computation of the Pareto set (which is intractable when many objectives are considered). On the other hand, this approach cannot identify the shape of the Pareto set, as is done in traditional multi-objective optimization and dimensionality reduction methods (Miettinen, 2012; Copado-Méndez et al., 2014).

The multi-stakeholder setting discussed here can be seen as a quasi-cooperative decision-making framework in which stakeholders have their own individual priorities expressed through the weights $\mathbf{w}_\omega$. A compromise solution for the stakeholders is found centrally (in a cooperative manner) by solving the CVaR minimization problem. We note that this approach yields a Pareto efficient solution while a fully decentralized approach (in which stakeholders do not reveal their priorities) does not. In particular, a decentralized setting often finds a game-theoretical equilibrium (e.g., a Nash equilibrium) which is not Pareto efficient. For more information on different decision-making settings arising in supply chains the reader is referred to (Garcia and You, 2015).

3.2. Network design

In addition to finding optimal allocation for resources, we often seek to identify optimal locations for different types of technologies (and associated capacities) to enhance operational performance. This problem is often referred to as the facility location or supply chain design problem.

Under the proposed modeling abstraction, we can formulate these *network design* problems by defining a set of candidate technology types $\mathcal{T}_\mathcal{N}$ that can be installed at a set (or subset) of predefined network nodes $\mathcal{N}$. We use the binary variable $y_{t,n} \in \{0, 1\}$ to indicate that technology t is installed at node n. Each technology $t \in \mathcal{T}_\mathcal{N}$ has a set of transformation factors $\gamma_{t,p}$, reference product $p'(t) = \texttt{prod\_tech}[t]$, capacity $\bar{g}_t = cap\_tech[t]$, and investment cost $\alpha_t^I := cost\_tech[t] \in \mathbb{R}_+$. The transformation factors $\gamma_{t,p}$ capture the consumption/generation of products $p \in \mathcal{P}$ in technology $t \in \mathcal{T}_\mathcal{N}$ and represent the amount of product p that is consumed/generated per unit of reference product $p'(t)$ consumed/generated.

We express the balance equations that capture all the possible technologies to be installed at node $n \in \mathcal{N}$ as:

$$\left(\sum_{i \in \mathcal{S}_{n,p}} s_i + \sum_{\ell \in \mathcal{F}_{n,p}^{in}} f_\ell \right) - \left(\sum_{j \in \mathcal{D}_{n,p}} d_j + \sum_{\ell \in \mathcal{F}_{n,p}^{out}} f_\ell \right) - \sum_{t \in \mathcal{T}_\mathcal{N}} \gamma_{t,p} r_{n,p'(t),t} = 0, (n, p) \in \mathcal{N} \times \mathcal{P}, \tag{3.18a}$$

$$\left(\sum_{i \in \mathcal{S}_{n,p'(t)}} s_i + \sum_{l \in \mathcal{F}_{n,p'(t)}^{in}} f_\ell \right) = \sum_{t \in \mathcal{T}_\mathcal{N}} (r_{n,p'(t),t} + u_{n,p'(t),t}), n \in \mathcal{N}, \tag{3.18b}$$

where $r_{n,p'(t),t}$ and $u_{n,p'(t),t}$ are the processed and unprocessed flows at node n, for technology t, and associated reference product $p'(t)$. We now introduce the logic that only one technology can be installed per node:

$$\sum_{t \in \mathcal{T}_\mathcal{N}} y_{t,n} = 1, n \in \mathcal{N}. \tag{3.19}$$

The processed flow of technology t is bounded by the capacity of the installed technology:

$$0 \le r_{n,p'(t),t} \le |\gamma_{n,p'(t)}| \cdot \bar{g}_t \cdot y_{t,n}, n \in \mathcal{N}, \quad t \in \mathcal{T}_\mathcal{N}. \tag{3.20}$$

This implicitly imposes a constraint on the generation/consumption flows for the technologies $g_{n,p'(t),t}$. The unprocessed flows $u_{n,p'(t),t}$ must satisfy:

$$0 \leq u_{n,p'(t),t} \leq \bar{u}_{n,p'(t),t} \cdot y_{t,n}, n \in \mathcal{N}, \quad t \in \mathcal{T}_{\mathcal{N}}, \tag{3.21}$$

where $\bar{u}_{n,p'(t),t}$ is a suitable upper bound.

In certain situations it is also of interest to consider the possibility of installing different types of technologies to transport products (e.g., a gas pipeline or a roadway). If we define the set of candidate transport technologies $\mathcal{T}_{\mathcal{F}}$, such a problem can be formulated in a straightforward manner by using the following set of constraints:

$$0 \leq f_\ell \leq \bar{f}_t \cdot w_{t,\ell}, \ell \in \mathcal{F}, \quad t \in \mathcal{T}_{\mathcal{F}}, \tag{3.22}$$

where the binary variable $w_{t,\ell} \in \{0, 1\}$ indicates that technology t is used in link ℓ. The flow is bounded by the technology capacity $\bar{f}_t$ and is zero otherwise.

Investment costs in design problems can easily be expressed in terms of the binary variables $y_{t,n}, w_{t,\ell}$. The design problem can thus be cast as the following multi-objective mixed-integer linear program (MILP):

$$\min\{\varphi_I, \varphi_j^d, \varphi_i^s, \varphi_\ell^f, \varphi_{n,p}^g\} \tag{3.23a}$$

$$\text{s. t. } (3.18) - 3.22). \tag{3.23b}$$

Here, the function φ_I captures total investment costs and $\varphi_j^d, \varphi_i^s, \varphi_\ell^f, \varphi_{n,p}^g$ capture operational costs/performance at every node. As before, we can compute compromise (Pareto) solutions for this problem by using prioritization (e.g., social welfare), multi-stakeholder formulations, or ϵ-constrained methods.

We highlight that the one-technology-per-node assumption is not as restrictive as it sounds because one can consider multiple technologies to be installed at the same geographical location by defining multiple nodes at the same location and by setting transportation costs between those nodes to zero.

In summary, the problem statement for the network design problem is as follows: Given a set of products ($\mathcal{P}$), sources ($\mathcal{S}$), sinks ($\mathcal{D}$), candidate locations ($\mathcal{N}$), and candidate technologies ($\mathcal{T}_{\mathcal{N}}$) the goal is to determine the locations ($y_{t,n}$) for placing these technologies, product flows (f_ℓ), and resource allocations (s_i and d_j) that constitute a Pareto optimal solution of problem (3.23).

4. Case studies

We illustrate the applicability of the proposed modeling framework by using case studies arising in the context of livestock organic waste management from concentrated animal feeding operations (CAFOs). Organic waste generated at U.S. CAFOs (manure) is estimated to be 300 million tons per year, which represents twice the amount of waste produced by the entire U.S. human population. A single dairy cow generates 20 tons/year of waste (MacDonald et al., 2009) and there are 9 million (Census of Agriculture, 2012) dairy cows in the U.S., which roughly translates to 180 million tons of waste generation each year. When organic waste is applied directly as fertilizer, it promotes phosphorus (P) accumulation in the soil, which can be lost as runoff to surface waters and trigger eutrophication. Eutrophication in turn leads to algal blooms which degrade water quality and disturb ecosystems. One strategy to mitigate eutrophication is to prevent P accumulation in an area of interest (i.e., balance P generation and intake from crops). This can be achieved by separating excess P from the waste and transporting it to P-deficient areas inside or outside the area of interest. Another environmental issue associated with manure is the emission of greenhouse gases (GHG) (methane and nitrous oxide) and of pathogenic bacteria. Capturing methane from waste (biogas) through anaerobic digestion provides an avenue to mitigate these issues. The U.S. Environmental Protection Agency (EPA) AgSTAR program reports that about 8000 U.S. farms could support biogas systems, providing about 1670 MW of electricity (enough to power one million homes) and reducing methane emissions by 1.8 million metric tons (in carbon dioxide equivalent this corresponds to taking 6.5 million cars off the road). The development of biogas and phosphorus recovery technologies has been historically difficult. According to the American Biogas Council, there are only 247 digester farm installations in the United States. A small number of P-recovering installations are also in operation. A reason for this is that deploying manure processing technologies is economically and logistically challenging. In particular, farms are highly dispersed geographically, which makes it challenging to balance economies of scale and transportation costs. Another issue is the need to capture the priorities of multiple stakeholders, which will seek to prioritize certain geographical regions (e.g., those with a higher concentration of P or those that are near to urban areas and watersheds) or that will seek to prioritize certain environmental objectives over others (e.g., water quality over GHG emissions).

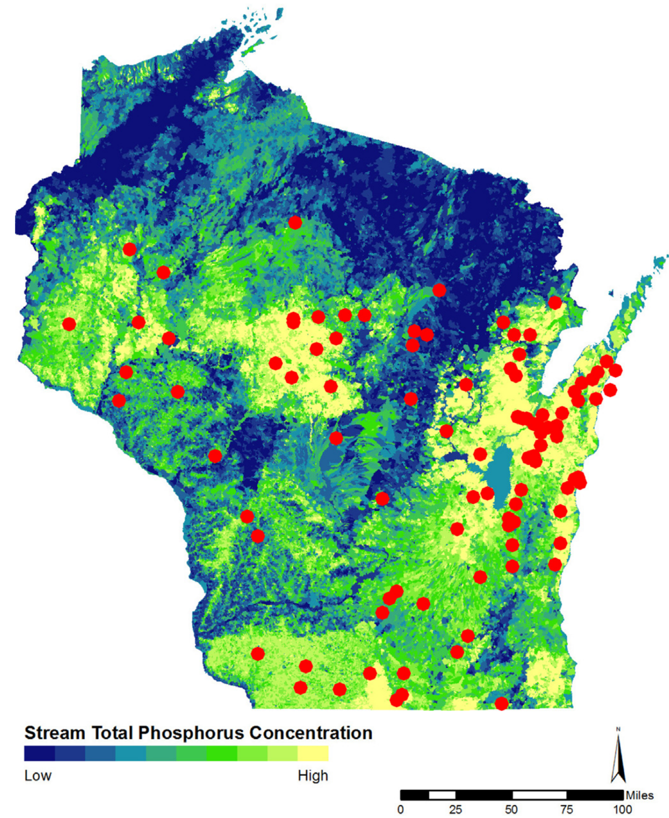

Fig. 3. Phosphorus concentration in the State of Wisconsin along with CAFOs locations.
Adapted from Wisconsin Integrated Assessment of Watershed Health (2014).

We use the proposed framework to determine optimal technology layouts for recovering phosphorus (in the form of struvite) and biogas from the dairy waste in the State of Wisconsin. Specifically, we seek to design a supply-chain network to process the organic waste of the 100 largest dairy farms (ranked by the number of animal units) in the state.[1] These farms act as sources of waste and also serve as candidate locations for installing the technologies. In Fig. 3 we present the CAFO locations and the soil P concentration in different regions of the state. As can be seen, there are *strong correlations between the CAFOs and phosphorus concentrations*.

[1] http://dnr.wi.gov/topic/AgBusiness/data/CAFO/cafo_all.asp.

Our studies seek to highlight conflicts that arise in these complex supply chain design studies and to highlight the insights that can be gained with the proposed framework. We consider the following specific cases:

- Phosphorus recovery analysis (without geographical priorities).
- Phosphorus recovery analysis (with geographical priorities).
- Phosphorus and biogas recovery analysis (with stakeholder priorities).

In summary, the scope of these case studies can be summarized as follows: given the data on 100 largest dairy CAFO locations (representing both the sources $s \in \mathcal{S}$ of waste and candidate locations $n \in \mathcal{N}$), candidate technologies ($t \in \mathcal{T}_{\mathcal{N}}$), their corresponding reference products ($p'(t)$), and transformation factors ($\gamma_{t,p}$), the goal is to identify Pareto optimal solutions for the placement of these technologies ($y_{t,n}$) and the product flows f_ℓ (corresponding to waste, struvite, digestate, and biogas) across the State of Wisconsin. This is achieved by maximizing the total amount of struvite recovered (Section 4.1), by maximizing struvite recovered by including geographical priorities (Section 4.2), and by minimizing the collective stakeholder dissatisfaction associated with different priorities on water quality and GHG impacts (Section 4.3).

4.1. Phosphorus recovery analysis

We consider three capacity variants for a P recovery technology in the form of struvite (magnesium ammonium phosphate $NH_4MgPO_4 \cdot 6H_2O$). Recovering P as struvite has the dual benefit of mitigating eutrophication and providing an alternative source to phosphate rock (obtained from mining). In Fig. 4 we present a simplified flowsheet for a fluidized bed reactor (FBR) technology used for recovering P as struvite. These reactors are commercialized by nutrient management companies such as Ostara (http://ostara.com). The capacity of the system considered is expressed in terms of the total amount of waste from animal units (AUs) that it can process. We consider processing capacities for 500, 1500, and 3000 AUs. A waste generation rate of 80 lbs/AU/day[2] is used to calculate the net waste generated by a farm, where AU denotes the number of animal units at each location. AU is a standard unit used in calculating the relative grazing impact of different classes of livestock. It is defined as an animal equivalent of 1000 pounds live weight. To provide a reference, a single dairy cow weighs about 1400 pounds or 1.4 AUs. In the study area, there are 280,567 AUs, which generate a total waste of 22,445,360 lb/day (about 10 million metric tons of waste per day).

The FBR technology takes waste as input to generate struvite and digestate as output products. We thus have the set of products $\mathcal{P}$:={*Waste*, *Struvite*, *Digestate*}. A recovery percentage of 6.47% for struvite from waste (on a per-mass basis) has been considered. This value is obtained by assuming that 90% of P (Cusick et al., 2014) present in the waste is recovered in the form of struvite. The generated digestate is used as a bedding material at animal farms and is assumed to represent the rest of the waste not recovered. The yield factors are summarized in the transformation matrix:

$$\begin{bmatrix} \textit{Technology} & \textit{Waste} & \textit{Struvite} & \textit{Digestate} \\ \textit{Str\_I} & -1 & 0.0647 & 0.9353 \\ \textit{Str\_II} & -1 & 0.0647 & 0.9353 \\ \textit{Str\_III} & -1 & 0.0647 & 0.9353 \end{bmatrix}$$

[2] https://www.nrcs.usda.gov/wps/portal/nrcs/detail/null/?cid=nrcs143_014211.

The capacities and investment costs for the technologies are given by:

$$\begin{bmatrix} \textit{Technology} & \textit{cap\_tech}(\text{kg/day}) & \textit{cost\_tech}(\text{USD}) & \textit{prod\_tech} \\ \textit{Str\_I} & 18,143 & 364,000 & \textit{Waste} \\ \textit{Str\_II} & 54,431 & 704,000 & \textit{Waste} \\ \textit{Str\_III} & 108,862 & 1,070,000 & \textit{Waste} \end{bmatrix}$$

The investment costs have been calculated by sizing the equipment units involved in the FBR process and then applying cost estimation techniques for the overall project (Walas, 1990; Peters et al., 2003). We consider a nominal design with a flow rate of Waste of 1 kg/s. The investment costs corresponding to the capacity equivalent of 500, 1500, and 3000 AUs (i.e., 0.21, 0.63 and 1.26 kg/s of Waste, respectively) are then estimated by using the *six-tenths-factor rule*, which captures economies of scale (Peters et al., 2003). The equipment units involved in the overall process are a mixing vessel, FBR, dryer, heat exchanger, and a hydrocyclone. The mixing vessel is used to make the waste uniform in composition. The cost of this vessel is estimated at 28,930 USD, which includes the material and agitator cost. The chemical formation of struvite occurs in the FBR according to the reaction:

$$Mg^{2+} + NH_4^+ + H_nPO_4^{n-3} + 6H_2O \rightarrow MgNH_4PO_4 \cdot 6H_2O + nH^+$$

The FBR is designed using bed design parameters reported in Jordaan (2011) and kinetic rate constants reported in Nelson et al. (2003). Using these values, we use standard design procedures (Kunii and Levenspiel, 1991) to estimate an equipment cost of 7225 USD. For the heat exchanger, dryer, and hydrocyclone we have estimated investment costs of 1916 USD, 121,014 USD, and 18,535 USD, respectively. The total equipment costs add up to 177,620 USD. The physical plant cost (which includes cost of pipes, equipment construction, buildings and site development) is calculated by multiplying the total equipment cost by a factor of 3.15 (Peters et al., 2003). The value obtained is then scaled up by a factor of 1.4 to obtain the total investment cost of 783,303 USD. This value is used to estimate the investment costs for the technology capacities.

The cost of transporting waste (via hauling trucks) is assumed to be 0.08 USD/km/ton (Paudel et al., 2009). For this case study, a value of 0.16 USD/km/ton is used in order to account for the two-way travel of the hauling trucks. The transport cost φ_ℓ^f factors in the distance traveled (in km) by the flows f_ℓ between the associated sending and receiving nodes. The per-unit transportation cost of digestate and struvite has been assumed to be same as that of transporting waste (i.e., the products use the same mode of transportation). The reference product is organic waste ($p'(t)$=$\texttt{Waste}$) for all the technologies (because these differ only in capacity).

We perform trade-off analysis among the conflicting objectives of maximizing total struvite recovered (denoted as $\varphi_{\texttt{str}}$) while minimizing total investment and transportation cost (denoted as $\varphi = \varphi_I + \varphi_f$). The cost is expressed on a per-day basis. We constrain this total cost by a budget level ϵ. In our analysis, we report percentage of unprocessed manure that remains in the system (denoted as ϕ_u). We also report the total number of technologies installed $\sum_{n,t} y_{n,t}$ and the average transportation distances for the waste (denoted as $h_{\texttt{Waste}}$) and struvite (denoted as $h_{\texttt{str}}$). Each farm has the option to treat the waste that it generates on-site or to transfer it to other locations. We use a common collection point for struvite at the boundary of the state in order to estimate the costs associated with shipping the recovered phosphorus out of the state (outside the network boundary) and with that prevent P accumulation in the state. This is modeled by defining a single demand for struvite at the collection point.

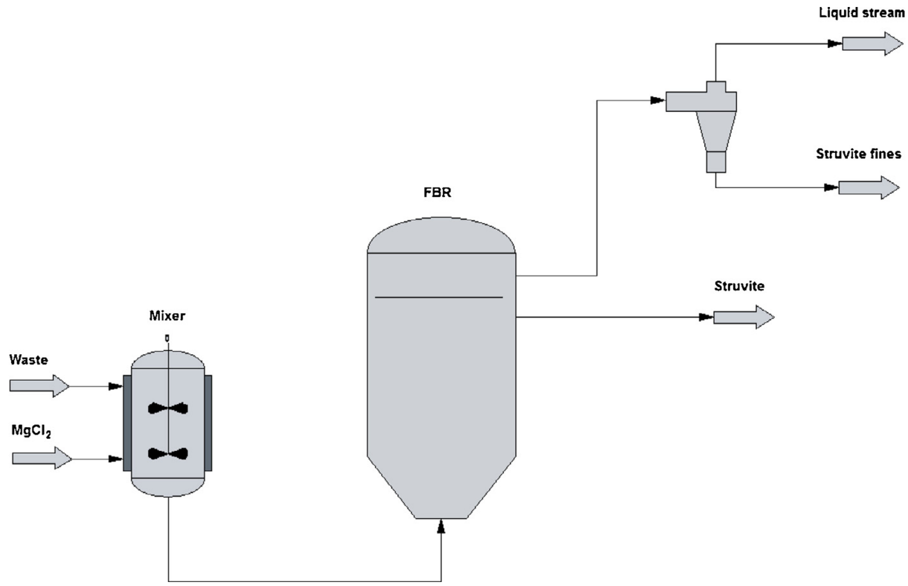

Fig. 4. Schematic of fluidized bed reactor process for recovery of P as struvite.

Table 1
Trade-off analysis results for struvite recovery study (without geographical priorities).

Budget (USD/day)	φ_I (USD)	φ_f (USD/day)	$\sum_{n,t} y_{n,t}$	$\varphi_{\texttt{str}}$ (kg/day)	ϕ_u (%)	$h_{\texttt{Waste}}$ (km/day)	$h_{\texttt{str}}$ (km/day)	$\varphi_{f,waste}$ (USD/day)	$\varphi_{f,str}$ (USD/day)
500,000	102.95×10^6	485,898	101	6.59×10^5	0.00	34.97	170.02	448,014	37,281
70,000	102.61×10^6	55,944	100	6.59×10^5	0.00	47.86	144.69	18,557	37,387
55,000	102.27×10^6	40,991	100	6.30×10^5	4.43	22.81	346.16	5342	35,649
45,000	93.60×10^6	32,179	96	5.59×10^5	15.13	7.21	341.99	818	31,361
35,000	75.10×10^6	24,713	77	4.53×10^5	31.27	6.81	328.29	532	24,181
25,000	57.30×10^6	17,151	59	3.41×10^5	48.18	6.72	300.44	405	16,746
15,000	38.38×10^6	9742	41	2.24×10^5	65.94	5.47	257.38	213	9530
10,000	28.78×10^6	6058	32	1.63×10^5	75.25	4.97	216.14	177	5881
5000	16.70×10^6	2713	18	0.95×10^5	85.57	0.95	164.58	25	2688
3000	11.01×10^6	1492	12	0.63×10^5	90.45	0.43	132.30	10	1481

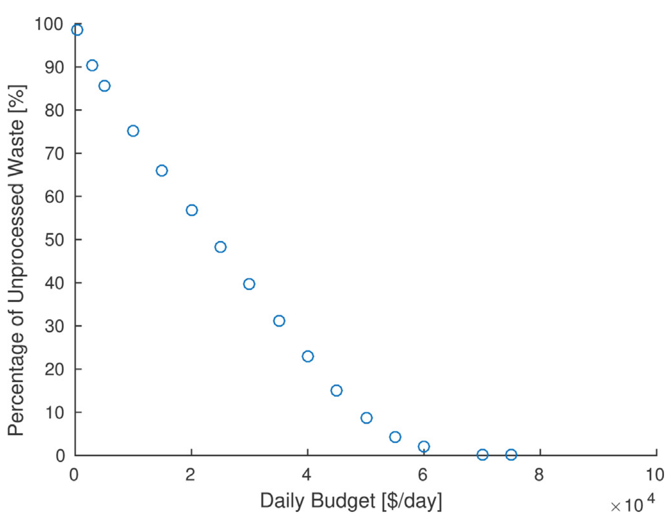

Fig. 5. Pareto curve for daily budget (daily cost) and percentage of unprocessed waste.

Table 1 summarizes the results of the trade-off analysis and Fig. 5 presents Pareto solutions for different budget levels. As expected, when the budget is unconstrained (we set the budget to a large value of 500,000 USD/day), the optimal supply chain consists of siting as many technologies as possible (101 facilities are installed) in order to treat all the waste present in the system (i.e., no waste is left untreated). As a result, the transportation costs and hauling distances are allowed to be arbitrarily large. This indicates that the model cannot distinguish between different locations and that the solution is degenerate (i.e., the same amount of struvite can be recovered regardless of the location). This degeneracy becomes evident when we reduce the budget to 70,000 USD/day. In this case, we obtain the same amount of struvite but the transportation costs are reduced by an order of magnitude. As we constrain the budget further, the investment cost remains the same but network flows are re-routed and transportation cost is reduced, indicating that there is some inherent flexibility in the supply chain that can be used to mitigate transportation costs. A further reduction in the budget value causes a fast increase in the amount of waste left unprocessed (a fast decrease in the total amount of struvite recovered). Interestingly, because the total mass of struvite recovered in each technology is just 6.47% of the total waste processed, it is *more economical to process the waste locally (at the source node) and then transport struvite to the collection point*. This is reflected in the average transporting distance for struvite $h_{\texttt{str}}$, which is much higher than that for waste $h_{\texttt{Waste}}$.

The left-hand side maps in Fig. 6 show the optimal supply chain configuration and associated flows for two budget cases. The red circles indicate the farm locations, the yellow ring indicates that a struvite recovery technology has been installed at that location, and the yellow circle represents the struvite collection point. The blue lines are organic waste flows and the yellow lines are struvite flows. We can see that, for the 55,000 USD/day budget case, there are manure exchanges across nodes so as to take full advantage of technology capacities. When the budget is reduced to 15,000 USD/day,

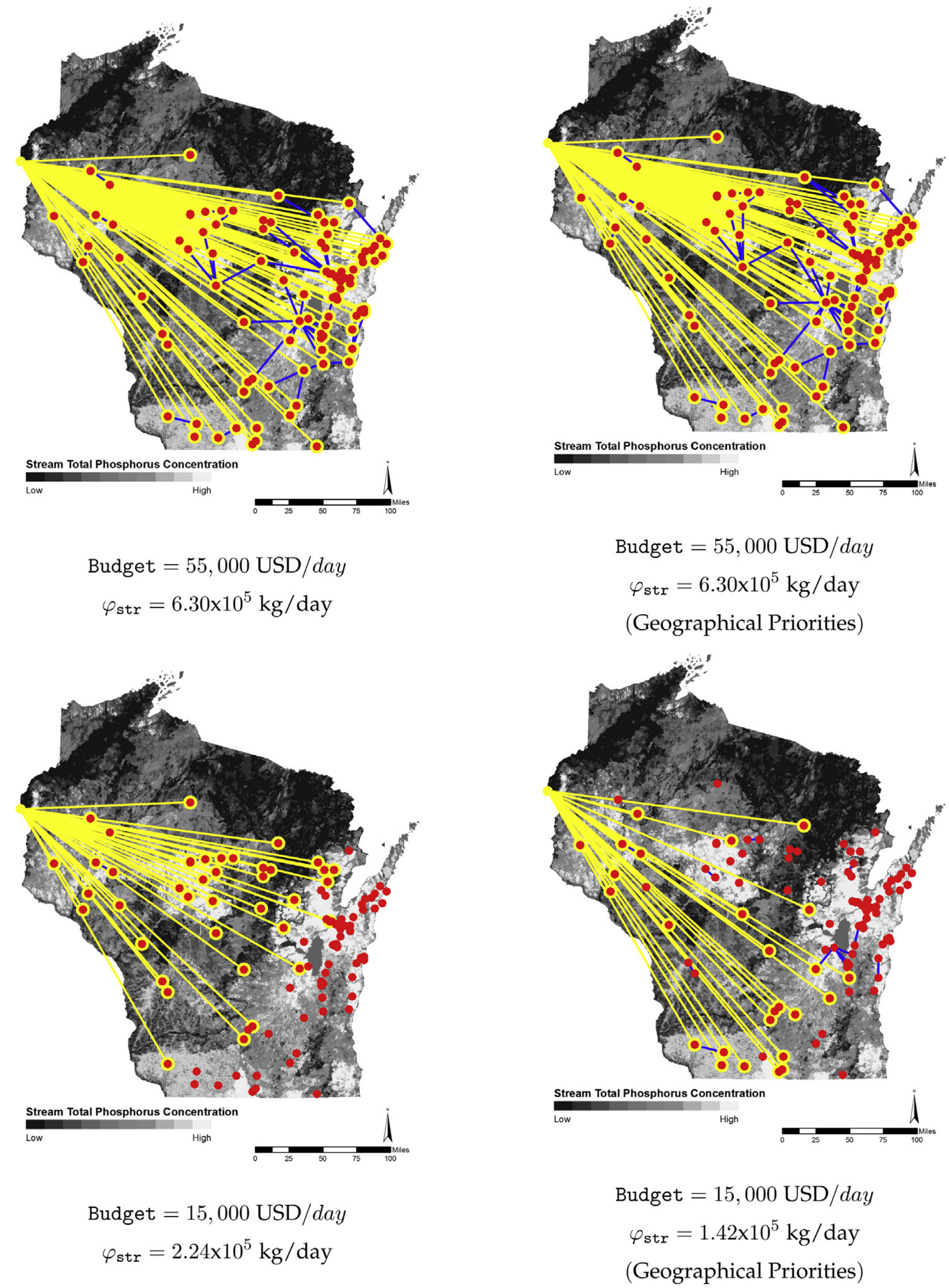

Fig. 6. Optimal technology locations and product flows under different budgets. (For interpretation of the references to color in this figure legend, the reader is referred to the web version of this article.)

it is more economical to treat all waste on-site and to transport struvite to the collection point. This is an indication that waste transportation costs dominate the budget. This is because the dairy waste has on average 87% water content by weight (MacDonald et al., 2009), while struvite produced in our case-study is water-free. Consequently, by treating the waste locally, the cost associated with transporting the associated water content can be saved.

4.2. Phosphorus recovery analysis (with geographical priorities)

From the tradeoff analysis shown in Table 1 we can see that, in order to process all the waste generated by the farms, *we would need an investment of over 100 million USD*. Under a constrained budget, it thus becomes important to prioritize geographical locations. We thus assign priorities to fields based on the existing soil P concentration at that location. In other words, we assign a higher priority to the waste generated at endangered areas. Under the proposed framework, this is done by making the waste supply cost α_i^s inversely proportional to the concentration of phosphorus at the corresponding location. In other words, a node with a high P concentration will supply waste at a lower cost and will thus have preference over other waste suppliers. Our objective is thus to maximize struvite demand delivered while minimizing supply waste cost (using the prioritized costs).

The results of this study are summarized in Table 2 and on the right-hand side maps of Fig. 6). We observe that, when the budget is 55,000 USD/day, the amount of struvite recovered (6.30×10^5 kg/day) is the same for both the cases. However, when the budget is reduced to 15,000 USD/day, the amount of struvite recovered for the case with priorities (1.42×10^5 kg/day) is less than

Table 2
Trade-off analysis results for struvite recovery study (with geographical priorities).

Budget (USD/day)	φ_I (USD)	φ_f (USD/day)	$\sum_{n,t} y_{n,t}$	$\varphi_{\mathtt{str}}$ (kg/day)	ϕ_u (%)	$h_{\mathtt{Waste}}$ (km/day)	$h_{\mathtt{str}}$ (km/day)	$\varphi_{f,waste}$ (USD/day)	$\varphi_{f,str}$ (USD/day)
500,000	102.60×10^6	485,944	101	6.59×10^5	0.00	33.63	92.97	441,619	41,925
70,000	103.31×10^6	55,848	101	6.59×10^5	0.00	46.58	217.95	18,625	37,223
55,000	101.90×10^6	41,040	100	6.30×10^5	4.51	21.51	346.19	5420	35,621
45,000	91.54×10^6	32,461	92	5.42×10^5	17.71	11.00	337.77	2405	30,055
35,000	74.05×10^6	24,856	75	4.26×10^5	35.32	10.81	321.42	2222	22,634
25,000	52.29×10^6	17,837	55	2.95×10^5	55.17	9.19	303.70	2805	15,032
15,000	25.96×10^6	11,444	27	1.42×10^5	78.48	11.13	282.45	4718	6725
10,000	15.97×10^6	7813	18	0.88×10^5	86.70	10.26	236.75	4228	3585
5000	4.62×10^6	4367	5	0.28×10^5	95.79	9.04	133.78	3623	745
3000	0.70×10^6	2904	1	0.04×10^5	99.47	7.98	74.08	2862	42

that recovered for the case without priorities (2.24×10^5 kg/day). This is because, when priorities are included, the supply chain focuses on processing waste at farms with high soil P concentration even if this comes at the expense of transporting the surplus waste from endangered areas over longer distances for treatment (and thus incurring higher costs). This can be visualized by comparing the maps in the right-hand side of Fig. 6. In particular, under prioritization, there is more movement of struvite in the supply chain. By comparing the left-hand and right-hand side maps we also see that, under a constrained budget, the technology locations are different (priorities do influence the supply chain design). On the other hand, under an unconstrained budget, there are no differences.

4.3. Phosphorus and biogas recovery

We now illustrate how to use the proposed framework to handle conflicting priorities among stakeholders. We consider a case study to locate technologies to recover both struvite and biogas. Stakeholders disagree on what product (struvite or biogas) should be prioritized. This setting can be interpreted as that of conflicting priorities from government officials or communities on using an available budget to address water quality (associated with P runoff) or air quality (associated with methane emissions). We compute compromise solutions for this problem by balancing the dissatisfactions of stakeholders.

We express the total struvite $\varphi_{\mathtt{str}}$ and biogas $\varphi_{\mathtt{bio}}$ recovered in terms of the demands served. Here, again, we assume that struvite is delivered to a single point (we consider a case with more collection points later on) and that biogas is delivered at the point of recovery (e.g., to fulfill local demands). Technologies `Str_I`, `Str_II`, and `Str_III` perform struvite recovery; technologies `Bio_I`, `Bio_II` and `Bio_III` perform biogas recovery; and technologies `BioStr_I`, `BioStr_II` and `BioStr_III` perform simultaneous struvite and biogas recovery. The corresponding data matrices for these technologies are:

$$\begin{bmatrix} \textit{Technology} & \textit{cap\_tech}(kg/day) & \textit{cost\_tech}(USD) & \textit{prod\_tech} \\ \textit{Str\_I} & 18,144 & 364,000 & \textit{Waste} \\ \textit{Str\_II} & 54,431 & 704,000 & \textit{Waste} \\ \textit{Str\_III} & 108,862 & 1,070,000 & \textit{Waste} \\ \textit{Bio\_I} & 18,144 & 574,509 & \textit{Waste} \\ \textit{Bio\_II} & 54,431 & 1,013,795 & \textit{Waste} \\ \textit{Bio\_III} & 108,862 & 1,672,723 & \textit{Waste} \\ \textit{BioStr\_I} & 18,144 & 938,509 & \textit{Waste} \\ \textit{BioStr\_II} & 54,431 & 1,717,795 & \textit{Waste} \\ \textit{BioStr\_III} & 108,862 & 2,742,723 & \textit{Waste} \end{bmatrix}$$

The investment cost for biogas recovery has been calculated using a general cost analysis formula reported by EPA's *AgStar* program (Meyer, 2011). For simplicity, the combined technology costs have been assumed to be the addition of the investment costs for the individual technologies. The transformation factors for the technologies (on a per mass basis) are given by:

$$\begin{bmatrix} \textit{Technology} & \textit{Waste} & \textit{Struvite} & \textit{Digestate} & \textit{Biogas} \\ \textit{Str\_I} & -1 & 0.0647 & 0.9353 & 0 \\ \textit{Str\_II} & -1 & 0.0647 & 0.9353 & 0 \\ \textit{Str\_III} & -1 & 0.0647 & 0.9353 & 0 \\ \textit{Bio\_I} & -1 & 0 & 0.96 & 0.04 \\ \textit{Bio\_II} & -1 & 0 & 0.96 & 0.04 \\ \textit{Bio\_III} & -1 & 0 & 0.96 & 0.04 \\ \textit{BioStr\_I} & -1 & 0.0621 & 0.8979 & 0.04 \\ \textit{BioStr\_II} & -1 & 0.0621 & 0.8979 & 0.04 \\ \textit{BioStr\_III} & -1 & 0.0621 & 0.8979 & 0.04 \end{bmatrix}$$

We consider a set of five different *types of stakeholders* that have different priorities on the product to be recovered. The first type of stakeholder has 100% preference on struvite recovery, the second type of stakeholder has 100% preference on biogas recovery, the third stakeholder is neutral, and the fourth and fifth stakeholders have biased preferences for struvite and biogas recovery, respectively. We can see that the first two types of stakeholders take extreme positions.

We begin our analysis by first reporting the ideal design for each stakeholder (those obtained by fully satisfying the priorities of each stakeholder). The results are presented in Table 3. As can be seen, there are strong trade-offs on the amount of products produced and on the associated investment and transportation costs. The supply chain layouts are shown in Fig. 7. As can be seen, the design of the first stakeholder type installs only struvite recovery technologies and requires transportation to the collection point (yellow circle). The design of the second stakeholder type only performs biogas recovery (blue rings) and does not require any transportation because biogas is consumed on-site. The third stakeholder type solution (with neutral priorities) is quite interesting and consists of installing struvite recovery facilities on one side of the state (close to the collection point) and biogas recovery facilities on the other side of the state. For this stakeholder, some facilities recover both biogas and struvite (green rings) and these are located in the middle of the state. This result implies that the location of the *collection point of struvite has a strong effect on the optimal configuration of the supply chain*. With such a diverse set of conflicting stakeholder designs, it becomes imperative to identify efficient compromise solutions.

Table 3
Ideal individual solutions for different stakeholder types.

Stakeholder	$w_{\mathtt{str}}$ (%)	$w_{\mathtt{bio}}$ (%)	$\varphi_{\mathtt{str}}$ (kg/day)	$\varphi_{\mathtt{bio}}$ (m^3/day)	φ_I (USD)	φ_f (USD/day)	$\varphi_{f,waste}$ (USD/day)	$\varphi_{f,str}$ (USD/day)
I	100	0	2.24×10^5	0.00	38.07×10^6	9786	278	9508
II	0	100	0.00	2.33×10^5	105.48×10^6	550	550	0
III	50	50	1.08×10^5	1.45×10^5	85.12×10^6	3340	109	3231
IV	33	67	3.38×10^3	2.30×10^5	104.82×10^6	641	600	41
V	67	33	2.24×10^5	0.00	38.41×10^6	9739	369	9370

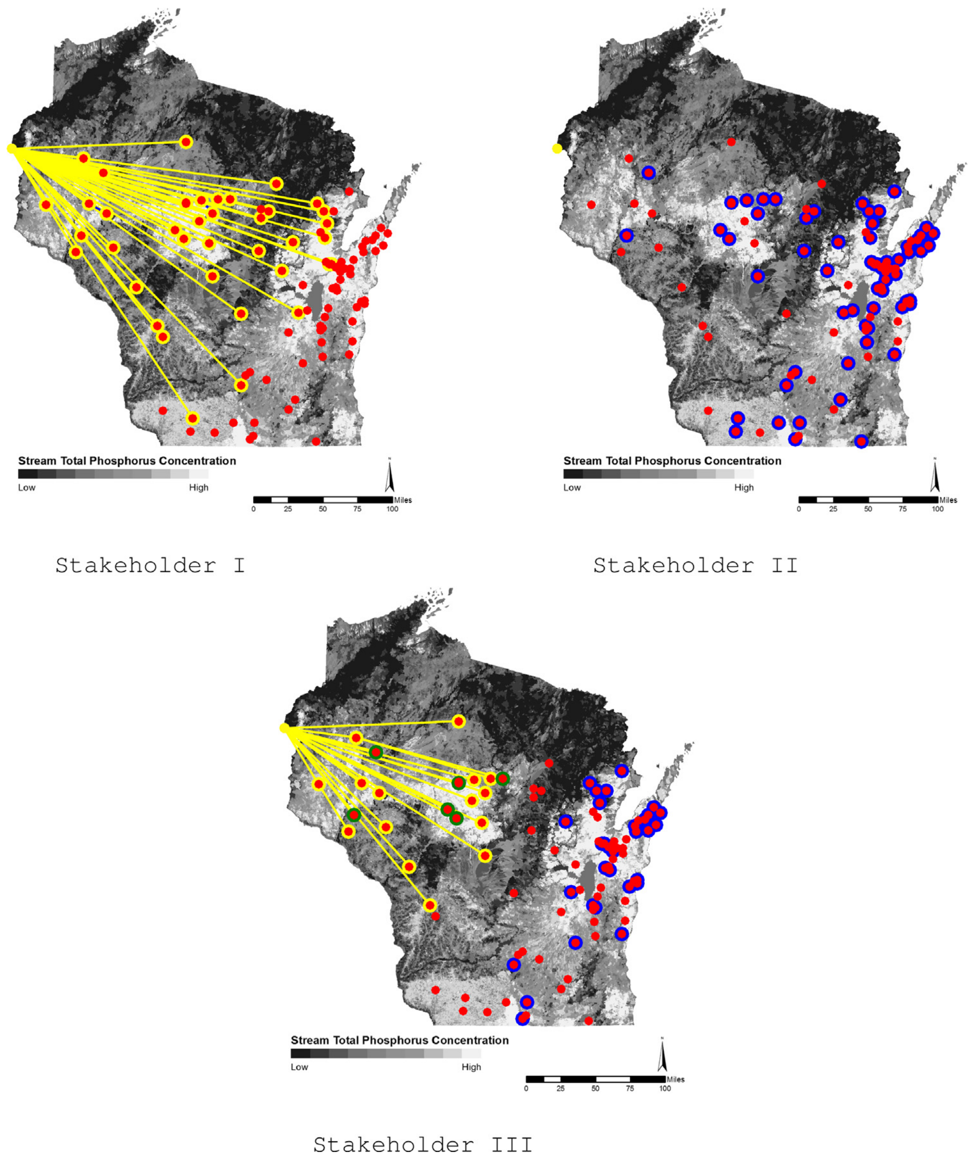

Fig. 7. Technology locations and flows for ideal stakeholder solutions.

Table 4
Costs and dissatisfactions under multi-stakeholder compromise solutions.

β	$\varphi_{\mathtt{str}}$ (kg/day)	$\varphi_{\mathtt{bio}}$ (m^3/day)	φ_I (USD)	φ_f (USD/day)	$\varphi_{f,waste}$ (USD/day)	$\varphi_{f,str}$ (USD/day)	d_I (%)	d_{II} (%)	d_{III} (%)	d_{IV} (%)	d_V (%)
0	1.24×10^5	1.29×10^5	79.47×10^6	4114	225	3889	45	45	0	12	12
0.5	1.25×10^5	1.29×10^5	79.23×10^6	4147	130	4017	46	43	0	11	12
0.7	1.22×10^5	1.32×10^5	80.54×10^6	3967	109	3858	47	42	0	11	13
1	1.07×10^5	1.45×10^5	84.41×10^6	3436	205	3231	54	35	0	8	15

In Table 4 we present the costs and dissatisfactions associated with each stakeholder type under different compromise solutions. In particular, we consider varying values of the probability level β and recall that $\beta = 0$ achieves a compromise in which the worst dissatisfaction is minimized and that a value of $\beta = 1$ achieves a compromise in which the average collective dissatisfaction is minimized. In Fig. 8 we present the optimal configuration for these two cases. As can be seen, the first two types of stakeholders are

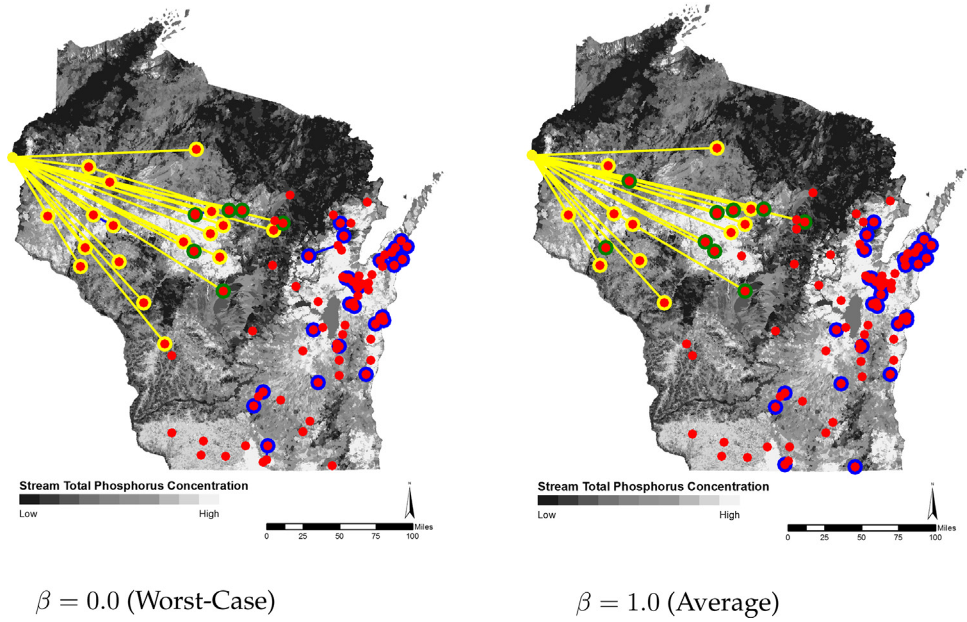

Fig. 8. Technology locations and flows for multi-stakeholder compromise solutions.

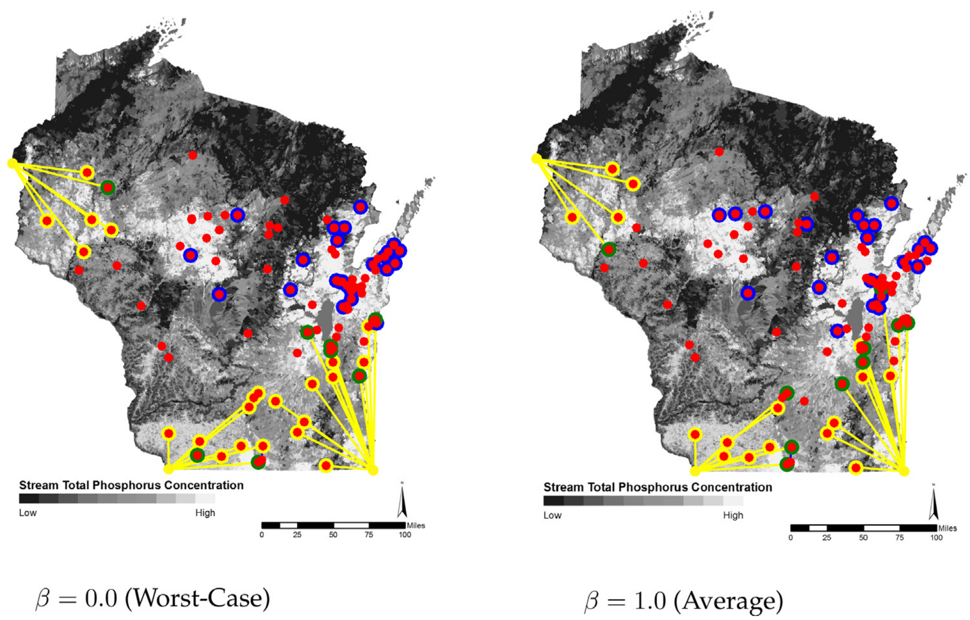

Fig. 9. Technology locations and flows for multi-stakeholder compromise solutions (for multiple collection sites).

the ones with the highest dissatisfactions (this is because they take extreme positions). Moreover, the first type of stakeholder (focusing on struvite) is the most dissatisfied. In particular, under the average compromise solution ($\beta = 1$), the first stakeholder type will be strongly dissatisfied compared to the rest while the worst-case compromise ($\beta = 0$) achieves a more even dissatisfaction among the stakeholders. Interestingly, in all cases the third stakeholder is fully satisfied with the compromise (its dissatisfaction is very small). This indicates that the compromise solutions are close to that of the neutral stakeholder.

We also observe that the worst-case compromise solution requires less investment but more transportation cost while the average compromise solution requires more investment but less transportation cost. This indicates that the worst-case compromise is seeking to satisfy the first stakeholder type by producing more struvite, even if this comes at the expense of more transportation costs to the collection point. On the other hand, the average compromise seeks to satisfy the second stakeholder and installs biogas facilities that use the fuel on-site, thus decreasing transportation cost. Such trade-offs are not perceptible from the configurations shown in Fig. 8. Here, the most evident difference is that the average compromise installs a few more technologies that perform joint recovery of biogas and struvite. Again, we see that the compromise solutions cluster biogas facilities on the east region of the state and struvite on the west region (close to the collection point). Again, this highlights that the collection point has a strong influence on the nature of the system layout. To reinforce this observation, in Fig. 9 we present optimal supply chain designs obtained from the stakeholder compromise solution when *multiple struvite collection points* are considered. As can be seen, the nature of the design changes drastically, with the struvite facilities now installed in the south and northwest regions of the state. These results indicate that the selection of collection points requires careful deliberations on the final use of struvite. The results also indicate that there exist complex trade-offs between the different types of environmental impact (water against air quality) that can result from deploying sub-optimal layouts. As a result, strong dissatisfactions will exist among stakeholders if facility locations are selected without carefully trading-off investment and transportation costs as well as geographical and stakeholder priorities.

4.4. Computational requirements

All the above optimization problems (MILPs) have been implemented in the algebraic modeling language `JuMP` and solved with the mixed-integer linear solver `Gurobi` on a computing server with 32 processor cores (2 sockets and 16 cores each) using Intel(R) Xeon(R) CPU E5-2698 v3 @ 2.30 GHz. The problem sizes range are: 300–900 binary variables, 30,000–42,000 continuous variables, 600–800 equality constraints, and 6000–18,000 inequality constraints. The CPU times range from a few seconds to one hour. The higher CPU times correspond to the instances where the investment budget constraints are tight (because of the increasing difficulty in finding a feasible solution).

5. Conclusions and future work

We have presented a general optimization formulation for multi-product supply chain networks. The formulation uses a general graph representation that considers a set of technologies placed at different spatially-dispersed nodes under which a set of products undergo transformations. Interactions between products are captured using a hierarchical graph that maps product flows at each node using a transformation matrix and that maps network nodes using transportation paths (arcs). The proposed network seeks to generalize a wide range of settings existing in the literature and to capture conflicting priorities. We demonstrate the applicability using a case study in the State of Wisconsin in which we seek to design supply chains to process livestock organic waste to mitigate phosphorus and methane emissions. The nature of the optimal layouts obtained indicates that complex trade-offs exist between investment, transportation, and environmental impact.

As part of future work, we are interested in exploring pricing properties resulting from the proposed network representation. In particular, the dual variables for the product balances can be interpreted as locational marginal prices for different products. We are also interested in using the framework to tackle more sophisticated case studies with time-dependent effects, more interdependent products and transportation alternatives, and different study areas.

Acknowledgments

We acknowledge funding from the National Science Foundation (under grant CBET-1604374) and MINECO (under grant DPI2015-67341-C2-1-R).

Appendix A. Nomenclature

Symbol	Description
Parameters	
prod_link[ℓ]	product associated with the flow through link $\ell \in \mathcal{F}$
cap_link[ℓ]	capacity limit for the flow through link $\ell \in \mathcal{F}$
cost_link[ℓ]	transportation cost for the flow through link $\ell \in \mathcal{F}$
snd_link[ℓ]	sending node associated with the flow through link $\ell \in \mathcal{F}$
rec_link[ℓ]	receiving node associated with the flow through link $\ell \in \mathcal{F}$
prod_src[i]	product associated with the source flow s_i
cap_src[i]	capacity of source $i \in \mathcal{S}$
node_src[i]	node associated with the source flow s_i
cost_src[i]	cost associated with the source flow s_i
prod_sink[j]	product associated with the sink flow d_j
cap_sink[j]	capacity of sink $j \in \mathcal{D}$
node_sink[j]	node associated with the sink flow d_j
cost_sink[j]	cost associated with the sink flow d_j
$\gamma_{n,p}$	transformation factor for product $p \in \mathcal{P}$ at node $n \in \mathcal{N}$
$p'(n)$:= refprod_node[n]	reference input product for node $n \in \mathcal{N}$
$\bar{g}_n$:=*cap_node*[n]	flow capacity for reference product $p'(n)$ at node $n \in \mathcal{N}$
$\bar{f}_\ell$	capacity limit for flow through link $\ell \in \mathcal{F}$
$\bar{s}_i$	capacity limit for source flow s_i
$\bar{d}_j$	capacity limit for sink flow d_j
α_j^d	per-unit demand cost at sink $j \in \mathcal{D}$
α_i^s	per-unit supply cost at source $i \in \mathcal{S}$
α_ℓ^f	per-unit transportation cost for flow through link $\ell \in \mathcal{F}$
$\alpha_{n,p}^g$	per-unit generation/consumption cost at node $n \in \mathcal{N}$
ϵ^d	threshold demand cost
ϵ^s	threshold supply cost
ϵ^f	threshold transportation cost
ϵ^g	threshold product generation/consumption cost
β	probability level for CVaR
$\gamma_{t,p}$	transformation factor for product $p \in \mathcal{P}$ at technology $t \in \mathcal{T}_\mathcal{N}$
$p'(t)$:= refprod_tech[t]	reference input product for technology $t \in \mathcal{T}_\mathcal{N}$
$\bar{g}_t$:=*cap_tech*[t]	flow capacity for reference product $p'(t)$ at technology $t \in \mathcal{T}_\mathcal{N}$
α_t^I:=*cost_tech*[t]	investment cost for technology $t \in \mathcal{T}_\mathcal{N}$
$\bar{u}_{n,p'(t),t}$	capacity limit for unprocessed flow of reference product $p'(t)$ corresponding to technology t through node n
Sets	
$\mathcal{N}$	nodes
$\mathcal{F}$	links (arcs)
$\mathcal{P}$	products
$\mathcal{S}$	out-of-network sources
$\mathcal{D}$	out-of-network sinks
$\mathcal{F}_n^{in}$	set of flows entering node $n \in \mathcal{N}$
$\mathcal{F}_n^{out}$	set of flows leaving node $n \in \mathcal{N}$
$\mathcal{F}_{n,p}^{in}$	set of flows of product $p \in \mathcal{P}$ entering node $n \in \mathcal{N}$
$\mathcal{F}_{n,p}^{out}$	set of flows of product $p \in \mathcal{P}$ leaving node $n \in \mathcal{N}$
$\mathcal{S}_n$	set of source flows to node $n \in \mathcal{N}$
$\mathcal{S}_{n,p}$	set of source flows of product $p \in \mathcal{P}$ to node $n \in \mathcal{N}$
$\mathcal{D}_n$	set of sink flows from node $n \in \mathcal{N}$
$\mathcal{D}_{n,p}$	set of sink flows of product $p \in \mathcal{P}$ from node $n \in \mathcal{N}$
Ω	set of stakeholders
$\mathcal{T}_\mathcal{N}$	candidate technologies
$\mathcal{T}_\mathcal{F}$	candidate transport technologies
Variables	
f_ℓ	flow associated with link $\ell \in \mathcal{F}$
s_i	flow associated with source $i \in \mathcal{S}$
d_j	flow associated with sink $j \in \mathcal{D}$
$g_{n,p}$	production flow for each product $p \in \mathcal{P}$ at node $n \in \mathcal{N}$
$r_{n,p'(n)}$	processed input flow for reference product p'(n) at node $n \in \mathcal{N}$
$u_{n,p'(n)}$	unprocessed input flow for reference product p'(n) at node $n \in \mathcal{N}$
φ_j^d	demand cost at sink $j \in \mathcal{D}$
φ_i^s	supply cost at source $i \in \mathcal{S}$
φ_ℓ^f	transportation cost for flow through link $\ell \in \mathcal{F}$
$\varphi_{n,p}^g$	generation/consumption cost of product $p \in \mathcal{P}$ at node $n \in \mathcal{N}$

φ^d	total demand cost over all sinks $j \in \mathcal{D}$
φ^s	total supply cost over all sources $i \in \mathcal{S}$
φ^f	total transportation cost over all links $\ell \in \mathcal{F}$
φ^g	total generation/consumption cost over all nodes and products $(n \times p) \in \mathcal{N} \times \mathcal{P}$
φ	social welfare function
$\mathbf{w}_\omega$	priority vector for stakeholder ω
f_ω	optimal objective for stakeholder ω
d_ω	dissatisfaction value for stakeholder ω
ν	value at risk
$y_{t,n}$	binary variable indicating if a technology t is installed at node n
$r_{n,p'(t),t}$	processed input flow for reference product $p'(t)$ at node n for technology t
$u_{n,p'(t),t}$	unprocessed input flow for reference product $p'(t)$ at node n for technology t
$w_{t,\ell}$	binary variable indicating if a technology t is used in link ℓ
ϕ	total investment and transportation cost (USD/day)
φ_I	total investment cost (USD)
$\varphi_{\mathtt{str}}$	total amount of struvite recovered (kg/day)
$\varphi_{f,str}$	total transportation cost for struvite (USD/day)
$\varphi_{f,bio}$	total transportation cost for biogas (USD/day)
$h_{\mathtt{waste}}$	average transportation distance for waste (km/day)
$h_{\mathtt{str}}$	average transportation distance for struvite (km/day)
ϕ_u	percentage of manure unprocessed (%)

List of acronyms

CAFO	concentrated animal feeding operation
CVaR	conditional value at risk
P	phosphorus
GHG	greenhouse gases
EPA	environmental Protection Agency
FBR	fluidized bed reactor
AU	animal unit

References

Čuček, L., Lam, H.L., Klemeš, J.J., Varbanov, P.S., Kravanja, Z., 2010. Synthesis of regional networks for the supply of energy and bioproducts. Clean Technol. Environ. Policy 12 (6), 635–645.

Čuček, L., Varbanov, P.S., Klemeš, J.J., Kravanja, Z., 2012. Total footprints-based multi-criteria optimisation of regional biomass energy supply chains. Energy 44 (1), 135–145.

Čuček, L., Martın, M., Grossmann, I.E., Kravanja, Z., 2014. Multi-period synthesis of optimally integrated biomass and bioenergy supply network. Comput. Chem. Eng. 66, 57–70.

2012 Census of Agriculture. Tech. Rep. USDA NASS. United States Department of Agriculture, National Agricultural Statistics Service.

Akgul, L.G., Zamboni, O., Bezzo, A., Shah, F., Papageorgiou, N., 2010. Optimization based approaches for bioethanol supply chains. Ind. Eng. Chem. Res., 4927–4938.

Akgul, O., Shah, N., Papageorgiou, L.G., 2012. Economic optimisation of a UK advanced biofuel supply chain. Biomass Bioenergy 41, 57–72.

Alex Marvin, W., Schmidt, L.D., Benjaafar, S., Tiffany, D.G., Daoutidis, P., 2012. Economic optimization of a lignocellulosic biomass-to-ethanol supply chain. Chem. Eng. Sci. 67 (1), 68–79.

An, H., Wilhelm, W.E., Searcy, S.W., 2011. A mathematical model to design a lignocellulosic biofuel supply chain system with a case study based on a region in Central Texas. Bioresour. Technol. 102 (17), 7860–7870.

Avami, A., 2012. A model for biodiesel supply chain: a case study in Iran. Renew. Sustain. Energy Rev. 16 (6), 4196–4203.

Balaman, S.Y., Selim, H., 2014. A network design model for biomass to energy supply chains with anaerobic digestion systems. Appl. Energy 130, 289–304.

Bloemhof-Ruwaard, J., Van Wassenhove, L., Gabel, H., Weaver, P., 1996. An environmental life cycle optimization model for the European pulp and paper industry. Omega 24 (6), 615–629.

Bowling, I.M., Ponce-Ortega, J.M., El-Halwagi, M.M., 2011. Facility location and supply chain optimization for a biorefinery. Ind. Eng. Chem. Res. 50 (10), 6276–6286.

Burak Aksoy, Harry Cullinan, David Webster, Kevin Gue, Sujith Sukumaran, Mario Eden Jr., N.S., 2011. Woody biomass and mill waste utilization opportunities in Alabama: transportation cost minimization, optimum facility location, economic feasibility, and impact. Environ. Prog. Sustain. Energy 30 (4), 720–732.

Chen, C.W., Fan, Y., 2012. Bioethanol supply chain system planning under supply and demand uncertainties. Transp. Res. Part E: Logist. Transp. Rev. 48 (1), 150–164.

Chen, X., 2014. An Economic Analysis of the Future U. S. Biofuel Industry, Facility Location, and Supply Chain Network.

Copado-Méndez, P.J., Guillén-Gosálbez, G., Jiménez, L., 2014. Milp-based decomposition algorithm for dimensionality reduction in multi-objective optimization: application to environmental and systems biology problems. Comput. Chem. Eng. 67, 137–147.

Corsano, G., Vecchietti, A.R., Montagna, J.M., 2011. Optimal design for sustainable bioethanol supply chain considering detailed plant performance model. Comput. Chem. Eng. 35 (8), 1384–1398.

Cusick, R.D., Ullery, M.L., Dempsey, B.A., Logan, B.E., 2014. Electrochemical struvite precipitation from digestate with a fluidized bed cathode microbial electrolysis cell. Water Res. 54, 297–306.

Dal-Mas, M., Giarola, S., Zamboni, A., Bezzo, F., 2011. Strategic design and investment capacity planning of the ethanol supply chain under price uncertainty. Biomass Bioenergy 35 (5), 2059–2071.

Dawoud, B., Amer, E., Gross, D., 2007. Experimental investigation of an adsorptive thermal energy storage. Int. J. Energy Res. 31, 135–147.

Dowling, A.W., Ruiz-Mercado, G., Zavala, V.M., 2016. A framework for multi-stakeholder decision-making and conflict resolution. Comput. Chem. Eng. 90, 136–150.

Dunnett, A., Adjiman, C., Shah, N., 2007. Biomass to heat supply chains applications of process optimization. Process Saf. Environ. Protect. 85 (5 B), 419–429.

Eksioglu, S.D., Acharya, A., Leightley, L.E., Arora, S., 2009. Analyzing the design and management of biomass-to-biorefinery supply chain. Comput. Ind. Eng. 57 (4), 1342–1352.

Elia, J.A., Baliban, R.C., Xiao, X., Floudas, C.A., 2011. Optimal energy supply network determination and life cycle analysis for hybrid coal, biomass, and natural gas to liquid (CBGTL) plants using carbon-based hydrogen production. Comput. Chem. Eng. 35 (8), 1399–1430.

Garcia, D.J., You, F., 2015. Supply chain design and optimization: challenges and opportunities. Comput. Chem. Eng. 81, 153–170.

Garcia, D.J., You, F., 2016. The water-energy-food nexus and process systems engineering: a new focus. Comput. Chem. Eng.

Giarola, S., Zamboni, A., Bezzo, F., 2011. Spatially explicit multi-objective optimisation for design and planning of hybrid first and second generation biorefineries. Comput. Chem. Eng. 35 (9), 1782–1797.

Grossmann, I.E., 2004. Challenges in the new millennium: product discovery and design, enterprise and supply chain optimization, global life cycle assessment. Comput. Chem. Eng. 29 (1), 29–39.

Guillén-Gosálbez, G., Grossmann, I.E., 2009. Optimal design and planning of sustainable chemical supply chains under uncertainty. AIChE J. 55 (1), 99–121.

Hu, T.C., 1963. Multi-commodity network flows. Oper. Res. 11 (3), 344–360.

Huang, Y., Chen, C.W., Fan, Y., 2010. Multistage optimization of the supply chains of biofuels. Transp. Res. Part E: Logist. Transp. Rev. 46 (6), 820–830.

Hugo, A., Pistikopoulos, E.N., 2005. Environmentally conscious long-range planning and design of supply chain networks. J. Clean. Prod.

Jordaan, E.M., 2011. Development of an Aerated Struvite Crystallization Reactor for Phosphorus Removal and Recovery from Swine Manure (Ph.D. thesis). University of Manitoba.

Kalaitzidou, M.A., Longinidis, P., Georgiadis, M.C., 2015. Optimal design of closed-loop supply chain networks with multifunctional nodes. Comput. Chem. Eng. 80, 73–91.

Kim, Y., Yun, C., Park, S.B., Park, S., Fan, L.T., 2008. An integrated model of supply network and production planning for multiple fuel products of multi-site refineries. Comput. Chem. Eng. 32 (11), 2529–2535.

Kim, J., Realff, M.J., Lee, J.H., 2011a. Optimal design and global sensitivity analysis of biomass supply chain networks for biofuels under uncertainty. Comput. Chem. Eng. 35 (9), 1738–1751.

Kim, J., Realff, M.J., Lee, J.H., Whittaker, C., Furtner, L., 2011b. Design of biomass processing network for biofuel production using an MILP model. Biomass Bioenergy 35 (2), 853–871.

Kunii, D., Levenspiel, O., 1991. Fluidization Engineering. Butterworth-Heinemann, Boston.

Lam, H.L., Varbanov, P.S., Klemeš, J.J., 2010. Optimisation of regional energy supply chains utilising renewables: P-graph approach. Comput. Chem. Eng. 34 (5), 782–792.

Leduc, S., Lundgren, J., Franklin, O., Dotzauer, E., 2010. Location of a biomass based methanol production plant: a dynamic problem in northern Sweden. Appl. Energy 87 (1), 68–75.

MacDonald, J., Ribaudo, M., Livingston, M., Beckman, J., Huang, W., 2009. Manure Use for Fertilzer and for Energy: Report to Congress.

Mele, F.D., Kostin, A.M., Guillén-Gosálbez, G., Jiménez, L., 2011. Multiobjective model for more sustainable fuel supply chains. A case study of the sugar cane industry in Argentina. Ind. Eng. Chem. Res. 50 (9), 4939–4958.

Meyer, D., 2011. Manure Treatment Technologies: Anaerobic Digesters. Tech. Rep. Agriculture and Natural Resources, University of California.

Miettinen, K., 2012. Nonlinear Multiobjective Optimization, vol. 12. Springer Science & Business Media.

Neiro, S.M.S., Pinto, J.M., 2004. A general modeling framework for the operational planning of petroleum supply chains. Comput. Chem. Eng. 28 (6–7), 871–896.

Nelson, N.O., Mikkelsen, R.L., Hesterberg, D.L., 2003. Struvite precipitation in anaerobic swine lagoon liquid: effect of ph and mg: P ratio and determination of rate constant. Bioresour. Technol. 89 (3), 229–236.

Papageorgiou, L., Rotstein, G., Shah, N., 2001. Strategic supply chain optimization for the pharmaceutical industries. Ind. Eng. Chem. Res. 40 (1), 275–286.

Papapostolou, C., Kondili, E., Kaldellis, J.K., 2011. Development and implementation of an optimisation model for biofuels supply chain. Energy 36 (10), 6019–6026.
Parker, N., Tittmann, P., Hart, Q., Nelson, R., Skog, K., Schmidt, A., Gray, E., Jenkins, B., 2010. Development of a biorefinery optimized biofuel supply curve for the Western United States. Biomass Bioenergy 34 (11), 1597–1607.
Paudel, K.P., Bhattarai, K., Gauthier, W.M., Hall, L.M., 2009. Geographic information systems (GIS) based model of dairy manure transportation and application with environmental quality consideration. Waste Manag. 29 (5), 1634–1643.
Peters, M.S., Timmerhaus, K.D., West, R.E., 2003. Plant Design and Economics for Chemical Engineers, vol. 4., 5th edition McGraw-Hill, New York.
Pritchard, G., Zakeri, G., Philpott, A., 2010. A single-settlement, energy-only electric power market for unpredictable and intermittent participants. Oper. Res. 58 (4-part-2), 1210–1219.
Santibañez-Aguilar, J.E., González-Campos, J.B., Ponce-Ortega, J.M., Serna-González, M., El-Halwagi, M.M., 2011. Optimal planning of a biomass conversion system considering economic and environmental aspects. Ind. Eng. Chem. Res. 50 (14), 8558–8570.
Tittmann, P.W., Parker, N.C., Hart, Q.J., Jenkins, B.M., 2010. A spatially explicit techno-economic model of bioenergy and biofuels production in California. J. Transp. Geogr. 18 (6), 715–728.
Varbanov, P., Friedler, F., 2008. P-graph methodology for cost-effective reduction of carbon emissions involving fuel cell combined cycles. Appl. Thermal Eng. 28 (16), 2020–2029.
Walas, S., 1990. Selection and Design Chemical Process Equipment. University of Kansas, USA.
Walther, G., Schatka, A., Spengler, T.S., 2012. Design of regional production networks for second generation synthetic bio-fuel – a case study in Northern Germany. Eur. J. Oper. Res. 218 (1), 280–292.
2014. Wisconsin Integrated Assessment of Watershed Health. Tech. Rep. March. U.S. Environmental Protection Agency.
You, F., Grossmann, I.E., 2008a. Design of responsive supply chains under demand uncertainty. Comput. Chem. Eng. 32 (12), 3090–3111.
You, F., Grossmann, I.E., 2008b. Mixed-integer nonlinear programming models and algorithms for large-scale supply chain design with stochastic inventory management. Ind. Eng. Chem. Res. 47 (20), 7802–7817.
You, F., Wang, B., 2011. Life cycle optimization of biomass-to-liquid supply chains with distributed-centralized processing networks. Ind. Eng. Chem. Res. 50 (17), 10102–10127.
You, F., Wassick, J.M., Grossmann, I.E., 2009. Risk management for a global supply chain planning under uncertainty: models and algorithms. AIChE J. 55, 931–946.
You, F., Tao, L., Graziano, D.J., Snyder, S.W., 2012. Optimal design of sustainable cellulosic biofuel supply chains: multiobjective optimization coupled with life cycle assessment and input–output analysis. AIChE J.
Zamboni, A., Shah, N., Bezzo, F., 2009. Spatially explicit static model for the strategic design of future bioethanol production systems. 2. Multi-objective environmental optimization. Energy Fuels 23 (10), 5134–5143.
Zavala, V.M., Kim, K., Anitescu, M., Birge, J., 2017. A stochastic electricity market clearing formulation with consistent pricing properties. Oper. Res., http://dx.doi.org/10.1287/opre.2016.1576.